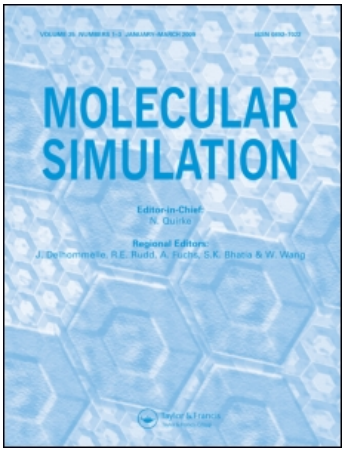

Molecular Simulation
Publication details, including instructions for authors and subscription information:
http://www.informaworld.com/smpp/title~content=t713644482

Electronic properties of poly(vinylidene fluoride): a density functional theory study

E. Ortiz[a]; A. Cuán[a]; C. Badillo[a]; C. M. Cortés-Romero[a]; Q. Wang[b]; L. Noreña[a]
[a] Basic Science and Materials Department, Metropolitan Autonomous University, Mexico City, Mexico
[b] Department of Materials Science and Engineering, The Pennsylvania State University, University Park, PA, USA

To cite this Article Ortiz, E. , Cuán, A. , Badillo, C. , Cortés-Romero, C. M. , Wang, Q. and Noreña, L.(2009) 'Electronic properties of poly(vinylidene fluoride): a density functional theory study', Molecular Simulation, 35: 6, 477 — 482
To link to this Article: DOI: 10.1080/08927020802680729
URL: http://dx.doi.org/10.1080/08927020802680729

Molecular Simulation
Vol. 35, No. 6, May 2009, 477–482

Taylor & Francis
Taylor & Francis Group

Electronic properties of poly(vinylidene fluoride): a density functional theory study

E. Ortiz[a]*, A. Cuán[a], C. Badillo[a], C.M. Cortés-Romero[a], Q. Wang[b] and L. Noreña[a]

[a]*Basic Science and Materials Department, Metropolitan Autonomous University, Azcapotzalco, Av. San Pablo 180, Col. Reynosa Tamaulipas, Mexico City 02200, Mexico;* [b]*Department of Materials Science and Engineering, The Pennsylvania State University, University Park, PA 16802, USA*

(*Received 31 October 2008; final version received 2 December 2008*)

We present a theoretical study of the piezoelectric polymer poly(vinylidene fluoride), PVDF. By density functional theory calculations, some of the distinct properties of this material have been obtained. Among such properties are hardness, capacitance, dipolar moment and energy associated with the conformational structural changes. For the calculations, we employed the B3LYP functional and the 6311 + G(d,p) basis set. Five chain molecules of varying length were studied, H—$(CH_2—CF_2)_x$—H, where $x = 1–4$ and 6 for the four different PVDF conformations, namely, I = T_p, II = TG_a, III = TG_p and IV = T_3G, where T means *trans* and G means *gauche*.

Keywords: theoretical study; PVDF; hardness; nanoscale capacitance

1. Introduction

Poly(vinylidene fluoride) (PVDF)-based polymers have been the focus of extensive research work due to their unique electrical properties: ferroelectric, piezoelectric and electroacoustic properties. Common dielectric materials may become polarised under an applied electrical field, whereas ferroelectric materials may become spontaneously polarised. Piezoelectric materials can transform a mechanical movement into an electric signal, and vice versa. On the other hand, electroacoustic materials can transform an acoustic wave into an electric signal, and vice versa. Several inorganic compounds are ferroelectric while PVDF is the only ferroelectric organic polymer known. Because of their light weight and easy processing and handling, PVDF-based polymers have potential applications in several new-technology electronics such as sensors, transducers, energy storage devices, communications and microphones [1]. Some applications currently under development include artificial muscles and harnessing energy from sea waves. However, only one of the four different PVDF conformations exhibits ferroelectric behaviour, the all-*trans* conformation or β-phase. The all-*trans*, all-T, conformation has a highly polarised backbone. The ferroelectric properties of PVDF can be enhanced by the introduction of trifluoroethylene, TrFE, as a co-monomer. P(VDF-TrFE) copolymers exhibit ferroelectric properties at TrFE contents between 50 and 85 mol % [2]. At a specific temperature, the Curie temperature, P(VDF-TrFE) copolymers show a conformational and phase transformation, from ferroelectric to paraelectric. The Curie temperature depends on the copolymer composition, and at this temperature the PVDF-based materials show some of the highest dielectric constants of any organic polymer, resulting from large crystalline polar domains. However, for energy storage applications, as in capacitors, a relatively high dielectric constant at room temperature and a smaller remnant polarisation [3] is more convenient, which can be accomplished by reducing the crystal domain size through high energy radiation or by the introduction of a third monomer, such as chlorotrifluoroethylene. Considerable effort has been devoted to understanding the structure–property relationships [4–15], but the mechanism and the phase stability and phase transitions are not yet completely elucidated. Quantum mechanics calculations can provide valuable information about the polarity and conformational energy states (also related to the Curie temperature) for several polymer compositions. The present contribution is focused on studying the variation in polarity, quantum capacitance and chemical hardness of a growing PVDF chain, together with the electronic properties.

2. Methodology

The electronic structure study includes all-electrons within the Kohn–Sham implementation of the density functional theory (DFT). The level of theory used in this work corresponds to the non-local hybrid functional developed by Becke, Lee–Yang–Parr (B3LYP) [16], whereas the Kohn–Sham orbitals are represented by a triple-ζ numerical with double polarised functions (d,p) plus one diffuse basis set; implemented in the Gaussian 03 code [17]. The electrostatic potential (ESP) method was used for the charge calculation [18]. The ESP charge

*Corresponding author. Email: meorv@correo.azc.uam.mx

ISSN 0892-7022 print/ISSN 1029-0435 online

DOI: 10.1080/08927020802680729
http://www.informaworld.com

calculation algorithm was chosen because it has no basis set dependence. Geometry optimisation calculations were carried out for all the involved systems using the Berny algorithm. The threshold convergence criterion was 10^{-6} a.u. for the energy, 0.000450 a.u. for the maximum force and 0.001800 a.u. for the maximum displacement. Five different-length chain molecules were studied, H—$(CH_2—CF_2)_x$—H, where $x = 1$, 2, 4, 6 for the four different PVDF conformations, namely, I = T_p, II = TG_a, III = TG_p and IV = T_3G, *vide* Figure 1. T means all-T, TG indicates TGTG′ and T_3G means TTTGTTG′, where T indicates *trans* and G means *gauche* conformation and the subindexes p and a correspond to polar phases with parallel dipoles and non-polar phases with anti-parallel dipole moments, respectively.

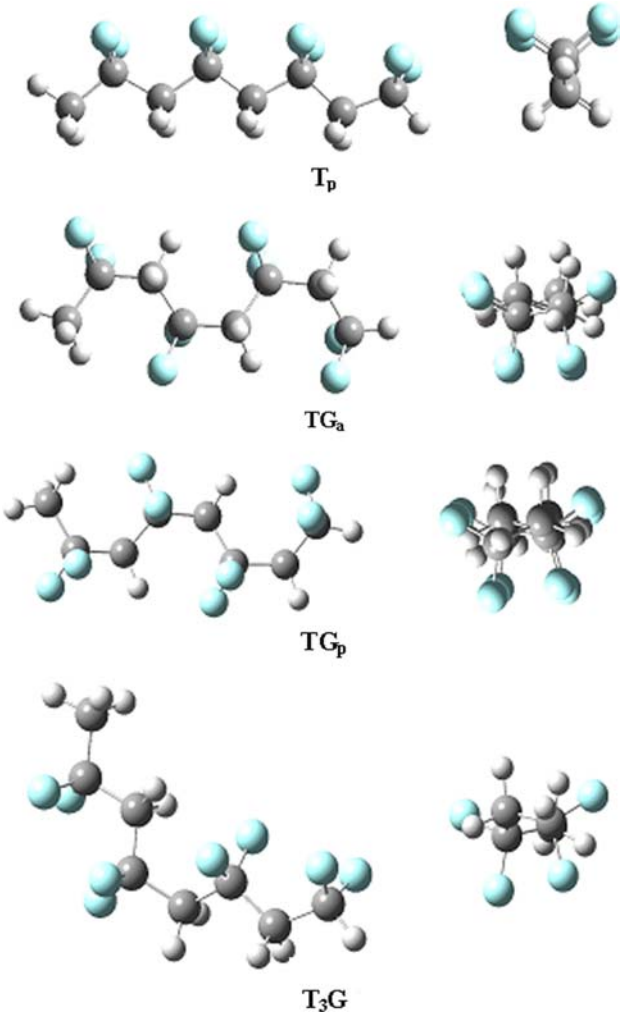

Figure 1. Structural representation for the different PVDF conformers, namely, T_p, TG_a, TG_p and T_3G. Fluorine atoms are in blue, carbon atoms are in grey and hydrogen atoms are in white.

2.1 Theoretical background

Electronegativity [19] (χ), and hardness [20] (η), for an N-electron system with total energy E, are defined as follows:

$$\chi = -\mu = -\left(\frac{\partial E}{\partial N}\right)_{v(\bar{r})}, \tag{1}$$

$$\eta = \frac{1}{2}\left(\frac{\partial^2 E}{\partial N^2}\right)_{v(\bar{r})} = \frac{1}{2}\left(\frac{\partial \mu}{\partial N}\right)_{v(\bar{r})}, \tag{2}$$

where μ and $v(\bar{r})$ are chemical and external potentials, respectively. The global softness (S) is the inverse of hardness [21],

$$S = \frac{1}{2\eta} = \left(\frac{\partial N}{\partial \mu}\right)_{v(\bar{r})}. \tag{3}$$

Using finite difference approximation for the small change in the number of particles, we can approximate μ, η and S as

$$\mu = -\left(\frac{\mathrm{IP} + \mathrm{EA}}{2}\right), \tag{4}$$

$$\eta = \frac{\mathrm{IP} - \mathrm{EA}}{2}, \tag{5}$$

$$S = \frac{1}{\mathrm{IP} - \mathrm{EA}}, \tag{6}$$

where IP is the ionisation potential and EA is the electron affinity.

The differential capacitance, C, of a charged system determines the specific amount of work per unit charge, ΔV, required to bring a fixed amount of charge, ΔQ, from the vacuum level to the system in question. As such

$$\frac{1}{C} = \frac{\Delta V}{\Delta Q}. \tag{7}$$

Macroscopically, capacitance is a system-specific quantity; it is dictated by the material characteristics of the system. For a conducting circular dot of radius R, filled with a material having a relative dielectric permittivity ε_r, the resulting classical capacitance is $C = 8\varepsilon_0\varepsilon_r R$.

From an atomistic viewpoint, and according to that reported in [22–24], there is a relationship between the chemical potential and ΔV, and after a mathematical procedure, through finite difference approximation, the capacitance of the system can be written as

$$\frac{e^2}{C_I(N)} = \mathrm{IP}(N) - \mathrm{EA}(N). \tag{8}$$

Note that $C_I(N)$ is considered to be a function of N, the total number of electrons in the system and IP(N) is

calculated as $E(N-1) - E(N)$; in the same way, EA(N) is obtained by $E(N) - E(N+1)$. Then, based on the Kohn–Sham approximation, the IP and the EA can be related to the E_{LUMO} and E_{HOMO} states for a N-particle system plus a constant; therefore Equation (8) can be written as

$$\frac{e^2}{C_I(N)} = E_{LUMO}(N) - E_{HOMO}(N) + B_0. \quad (9)$$

On the other hand, making use of the hardness global descriptor, it is possible to take a simple alternative, a direct approach for connecting the dimensions of quantum systems and their energetics. This approach takes advantage of the principles of electrostatics and a developing body of evidence that atoms and molecules or even nanoparticles behave much like macroscopic spherical capacitors, with specific shapes and capacities. It has been demonstrated by Ellenbogen et al. [25] that quantum capacitances of non-spherical, rod-like molecular wires can be approximated by a linear law that classical spherical capacitors follow. This linear isoperimetric [26] scaling law for the capacitances leads to a simple formula that relates a molecule's difficult-to-calculate EA directly to its IP and spatial dimensions. Therefore, following Iafrate et al. [22], as well as Gazquez and Ortiz [27], Perdew [28], and Sabin et al. [23], the capacitance of an atom or molecule may be evaluated as

$$C_I = \frac{1}{(IP - EA)} = \frac{1}{2\eta}. \quad (10)$$

3. Results and discussion

In order to understand the relationship between chemical and electrical properties of the PVDF material, we performed the torsion of the dihedral angle of two monomer units, *vide* Figure 2. Following the dihedral angle torsion of the G-to-T geometry transformation, the potential energy surface (PES) gives the relative energies and structural changes among them. Figure 2 shows that the TG_a, TG_p and T_p are stable geometric conformations because all of them are situated at minimum positions within the PES. In this case, the TG phases are energetically more stable than the T_p phase. According to Figure 2, reaching the T_p conformation requires a large energy supply. Barrier 2 (Barr2) indicates the amount of energy to reach T_p from TG_p and it is around of 4 kcal/mol (16.74 kJ/mol), which is in agreement with that reported elsewhere [29], and the energy difference between them is about 2.35 kcal/mol (9.83 kJ/mol). Based on the computed results, the energy barrier for converting the TG_a into the TG_p structural conformation is about 2.1 kcal/mol (8.79 kJ/mol); this means half of the energy is required to reach the T_p structural conformation, as it can be observed in Figure 2. Therefore, even if the T_p conformation has a higher energy level with respect to TG conformations, once the energetic barrier may be overcome, a stable structure is obtained. These structural conformations are directly related to a corresponding phase in the crystal.

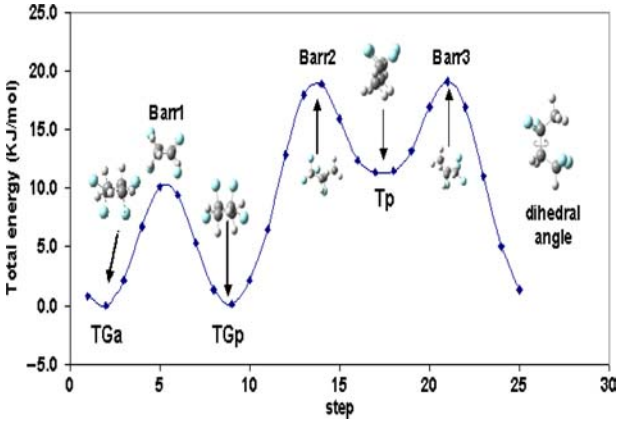

Figure 2. Graphical representation of the surface potential energy for the dihedral angle torsion showed on the right side of the picture. This graph displays the energy associated with the different structural conformations, namely, TG_a, TG_p and T_p.

We shall bear in mind that the molecular energy computed in this simplified model is far away from that of the real crystal; nevertheless, computing simulations are consistent with the available experimental observations [27].

The analysis of the differences among the structural changes obtained along the PES in Figure 2 leads to the values in Table 1, where some electronic properties and their corresponding values are presented. Considering only two monomer units, i.e. $n_r = 4$, where n is the total number of carbon atoms in the structure, the computed results indicate that the dipole moment of the T_p conformation is approximately 40% higher than that of the rest of the structural conformations (TG_a, TG_p and T_3G). The dipole moment of the different conformations is presented in Figure 3. The blue line corresponds to the dipole moment variation depending on the chain length of the T_p conformation. Similarly, the green line corresponds to the TG (a or p) conformation and the orange line corresponds to the T_3G phase. In general, the picture shows that the dipole moment increases as the length of the carbon chain increases. The T_p conformation exhibits the larger increase in the dipole moment. The TG structural conformation shows an intermediate increase whereas the T_3G conformational phase has the lowest one. The dipole moment increase for T_p is about 40% stronger than the TG's conformations and 55% stronger than the T_3G conformation. This means that the structural arrangement of the T_p phase promotes an increase in the polarity of the system, as already known. The charge polarisation can also be obtained (*vide* Figure 4), where the positive and negative ESP charges in the T_p conformation are perfectly

Table 1. IP and EA, hardness (η), quantum molecular capacitance (C_I) and dipole moment for the different PVDF structural conformations.

No. of C atoms n_r	Length L (Å)	− IP E_{HOMO} (eV)	EA E_{LUMO} (eV)	ΔE [a] (eV)	η (eV)	C_I (eV^{-1})	Dipole (D)
T_p							
2	3.30	−9.63	0.08	9.72	4.77	0.105	2.52
4	5.62	−9.24	−0.33	8.91	4.78	0.105	4.68
6	8.17	−9.08	−0.58	8.50	4.83	0.104	6.74
8	10.68	−8.99	−0.75	8.25	4.87	0.103	8.76
12	15.63	−8.93	−0.95	7.98	4.94	0.101	12.70
TG_a							
2	3.30	−9.63	0.08	9.72	4.77	0.105	2.52
4	5.25	−9.57	−0.19	9.38	4.88	0.103	2.37
6	7.62	−9.47	−0.37	9.11	4.92	0.102	4.30
8	9.86	−9.41	−0.46	8.95	4.93	0.101	5.04
12	14.43	−9.30	−0.57	8.72	4.94	0.101	7.97
TG_p							
2	3.30	−9.63	0.08	9.72	4.77	0.105	2.52
4	5.26	−9.56	−0.07	9.49	4.81	0.104	2.55
6	7.62	−9.48	−0.48	9.01	4.98	0.100	4.08
8	9.86	−9.42	−0.57	8.84	4.99	0.100	4.73
12	14.43	−9.31	−0.70	8.605	5.01	0.100	7.57
T_3G							
2	3.30	−9.63	0.08	9.72	4.77	0.105	2.52
4	5.26	−9.57	−0.19	9.38	4.88	0.102	2.36
6	6.75	−9.38	−0.49	8.89	4.93	0.101	3.32
8	9.90	−9.19	−0.56	8.632	4.88	0.103	3.64

[a] $\Delta E = E_{LUMO} - E_{HOMO}$.

ordered at the outside part of the molecule. The TG's and T_3G conformational systems do not show the same split charge distribution.

Hence, the dipole variation and the charge polarisation of the T_p system are characteristic of a ferroelectric material; they together act to form an electric dipole moment even in the absence of an external electrical field, as it is currently demonstrated. Moreover, the simple molecular model in Figure 2 shows that the energy barriers among the different structural conformations are not too high to avoid switching among them with a relatively low energy supply. All these additive properties present in the T_p structure may produce a ferroelectric material when the system size enlarges to a polymer crystal. The IR spectra

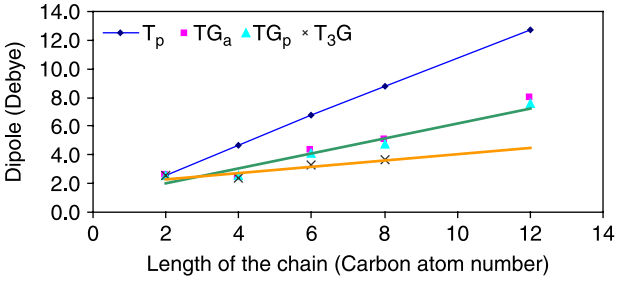

Figure 3. Dipole moment trend (in Debye) for the different PVDF structural conformations. In blue for T_p, in green for TG_a and TG_p and in orange for T_3G.

of all the conformations has been previously calculated [29], and we have obtained the same band distribution, namely: a first band from the C—H stretching mode with a relative weak intensity at approximately 3000 cm^{-1}, a second band with higher relative intensity corresponding to the C—H rocking mode between 1400 and 1500 cm^{-1}, which matches well with the experimental results (1362–1462 cm^{-1}). A relative weak third band at 1000–1350 cm^{-1} for CH twisting and wagging modes, and a fourth band from 700 to 950 cm^{-1} mainly associated with —CH_2 and —CF_2 rocking and skeletal bending vibrational modes. For further details, see [29].

So far, the current results for the model's representation give a good description of the system, also in line with the literature reported previously. Furthermore, some additional parameters can be presented. The hardness and the quantum capacitance indexes, C_I, calculated with the present DFT scheme remained almost invariable throughout the growing molecular system, *vide* Table 1. These nearly constant values contribute to the switching facility between the different structural conformations. The hardness, η, is inversely related to the quantum capacitance, C_I.

Figures 5 and 6 show the electronic states distribution of the valence band and the conduction band for the T_p and TG_p conformers, respectively. We can observe that the band gap between the valence and the conduction bands decreases as the total number of carbon atoms increases; being shorter in the T_p conformer than in the TG_p

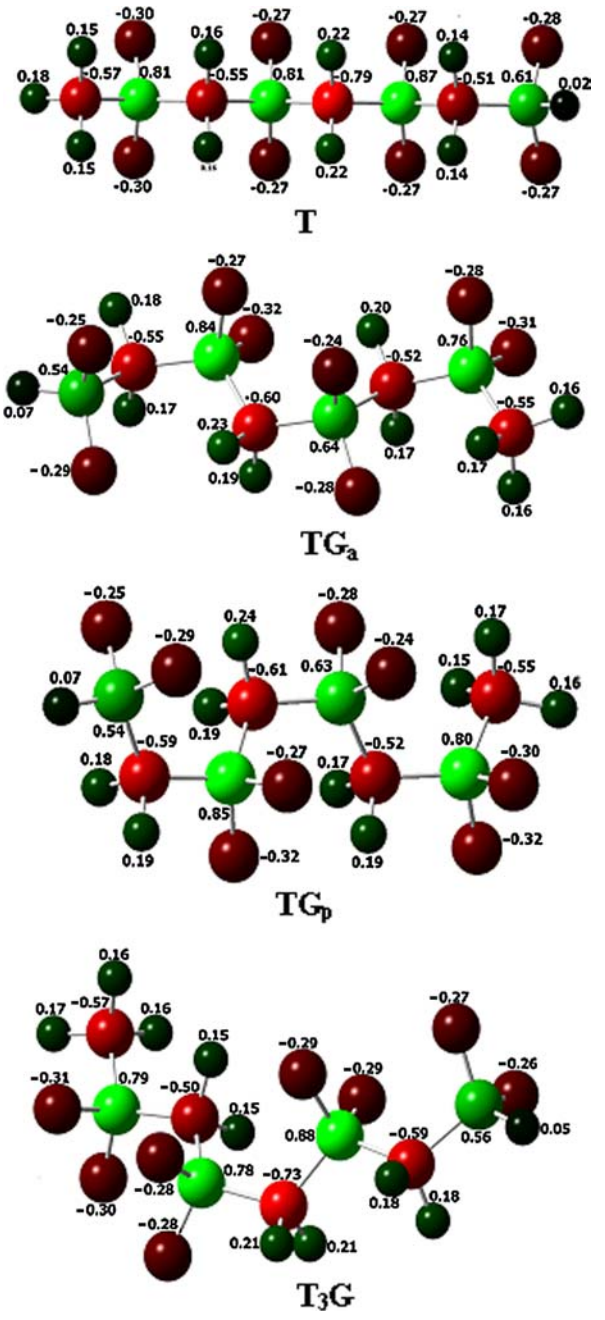

Figure 4. ESP charge representation for T_p, TG_a, TG_p and T_3G. Negative charge values are in red, positive charge values are in dark green and the larger positive charges are depicted in light green.

conformer. The number of empty molecular orbitals under the Fermi level increases as the length of the chain also increases. Therefore, the |HOMO − LUMO| energy difference also exhibits a decrease, being highly notorious for the T_p conformer. In the T_p conformer, there is a noticeable increase of the empty states under the Fermi level. Although, the reduction in the |HOMO − LUMO| band gap is low, whereas the conduction band lies

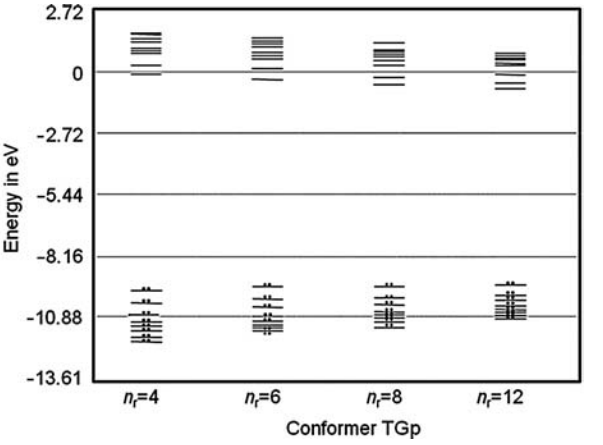

Figure 5. Electronic states distribution for the valence and conduction bands for the T_p conformer with $n_r = 4$, 6, 8 and 12 carbon atoms forming the structure.

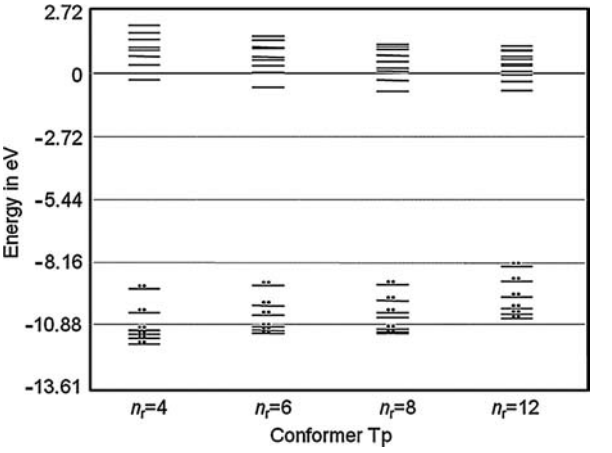

Figure 6. Electronic states distribution for the valence and conduction bands for the TG_p conformer with $n_r = 4$, 6, 8 and 12 carbon atoms forming the structure.

sufficiently low for rendering a negative band gap value, corresponding to a semimetal behaviour.

4. Conclusions

The quantum mechanics calculations of the energetics and structures corresponding to the different PVDF structural conformations show that the T_p conformation is energetically stabilised. The changes in the molecular arrangement associated with T_p, TG_a or TG_p and T_3G conformations led to significant changes in shape and electrical–chemical properties. A larger dipole moment and orientational charge polarisation were obtained for the all-*trans* T_p molecular structure, which can be obtained by the accumulative motion of the neighbouring groups, through large-scale T–G conformational changes. The dipole moment increase and the charge polarisation

in the T_p system are characteristics of a ferroelectric material. These contribute to form an electric dipole moment, even in the absence of an external electrical field. The molecular model shows that the energy barriers among the different structural conformations are not too high, allowing to switch among them with a relatively low energy supply. The interphase mobility among the different conformations is an important property for actuators. From our calculations, it is also demonstrated that the energy of the T_p empty states decreases under the Fermi level as the chain length increases, indicating that the resulting oligomer and the final polymer will have different electronic properties enhancing the electrical conductivity. All these additive properties of the T_p structure model may produce a ferroelectric material when the system size scales up to a polymer crystal.

Acknowledgements

A. Cuán, C. Badillo and Cortés-Romero are grateful for the sponsorship from CONACYT. A. Cuán thanks SEP-CONACYT for financial support through the project 80361. We gratefully acknowledge the financial support from PROMEP and from the Basic Science Department, UAM-A. E. Ortiz and L. Noreña thank PROMEP and SEP-CONACYT for the distinction and support for the SNI membership.

References

[1] S.B. Lang and S. Muensit, *Review of some lesser known applications of piezoelectric and pyroelectric polymers*, Appl. Phys. A 85 (2006), pp. 125–134.

[2] Y. Lu, J. Claude, Q.M. Zhang, and Q. Wang, *Microstructures and dielectric properties of the ferroelectric fluoropolymers synthesized via reductive dechlorination of poly(vinylidene fluoride-co-chlorotrifluoroethylene)*, Macromolecules 39 (2006), pp. 6962–6968.

[3] B. Chu, X. Zhou, K. Ren, B. Neese, M. Lin, Q. Wang, F. Bauer, and Q.M. Zhang, *A dielectric polymer with high electric energy density and fast discharge speed*, Science 313 (2006), pp. 334–336.

[4] J. Xu, M. Johnson, and G.L. Wilkes, *A tubular film extrusion of poly(vinylidene fluoride): structure/process/property behavior as a function of molecular weight*, Polymer 45 (2004), pp. 5327–5340.

[5] A.J. Lovinger, D.D. Davis, R.E. Cais, and J.M. Kometani, *The role of molecular defects on the structure and phase transitions of poly(vinylidene fluoride)*, Polymer 28 (1987), pp. 617–626.

[6] R. Hasegawa, M. Kobayashi, and H. Tadokoro, *Molecular conformation and packing of poly(vinylidene fluoride). Stability of three crystalline forms and the effect of high pressure*, Polym. J. 3 (1972), pp. 591–605.

[7] N. Takahashi, *Molecular dynamics simulation of electrostatic structural phase transition in ferroelectric poly(vinylidene fluoride)*, Jpn. J. Appl. Phys. 35 (1996), pp. 688–693.

[8] N. Karasawa and W.A. Goddard, *Force, fields, structures and properties of poly(vinylidenefluoride) crystals*, Macromolecules 25 (1992), pp. 7268–7281.

[9] J.C. Li, C.L. Wang, W.L. Zhang, X.X. Yan, and Y.X. Wang, *Vibrational modes analysis of poly(vinylidene fluoride-trifluoroethylene)*, Acta Phys. Sin. 51(4) (2002), pp. 776–781.

[10] C.L. Wang, J.C. Li, W.L. Zhong, and P.L. Zhang, *IR vibrational modes of PVDF chains*, Synth. Met. (2003), pp. 135–136, 469–470.

[11] J.C. Li, C.L. Wang, W.L. Zhong, P.L. Zhang, Q.H. Wang, and J.F. Webb, *Vibrational mode analysis of ß-phase poly(vinylidene fluoride)*, Appl. Phys. Lett. 81(12) (2002), pp. 2223–2225.

[12] B.L. Farmer, A.J. Hopfinger, and J.B. Lando, *Effect of trifluoroethylene monomers on molecular conformation of poly (vinylidene fluoridetrifluoroethylene) copolymer*, J. Appl. Phys. 43 (1972), pp. 4293–4303.

[13] H.M.G. Correia and M.M.D. Ramos, *Quantum modelling of poly(vinylidene fluoride)*, Comput. Mater. Sci. 33 (2005), pp. 224–229.

[14] T. Furukawa, *Ferroelectric properties of vinylidene fluoride copolymers*, Phase Transit. 18 (1989), pp. 143–211.

[15] K. Tashiro and M. Kobayashi, *Structural phase transition in ferroelectric fluorine polymers: X-ray diffraction and infrared/ Raman spectroscopic study*, Phase Transit. 18 (1989), pp. 213–246.

[16] (a) A.D. Becke, *Density-functional thermochemistry. III. The role of exact exchange*, J. Chem. Phys. 98 (1993), pp. 5648–5653. (b) C. Lee, W. Yang, R.G. Parr, *Development of the Colle-Salvetti correlation-energy formula into a functional of the electron density*, Phys. Rev. B 37 (1988) pp. 785–789.

[17] M.J. Frisch, G.W. Trucks, H.B. Schlegel, G.E. Scuseria, M.A. Robb, J.R. Cheeseman, J.A. Montgomery Jr., T. Vreven, K.N. Kudin, J.C. Burant, et al., *Gaussian 03, Revision C.02*, Gaussian, Inc., Wallingford, CT, 2004.

[18] B.H. Brent, K.M. Merz, Jr., and P.A. Kollman, *Atomic charges derived from semiempirical methods*, J. Comput. Chem. 11 (1990), pp. 431–439.

[19] R.G. Parr, D.A. Donnelly, M. Levy, and W.E. Palke, *Electronegativity – the density functional viewpoint*, J. Chem. Phys. 68 (1978), pp. 3801–3807.

[20] R.G. Parr and R.G. Pearson, *Absolute hardness: comparison parameter to absolute electronegativity*, J. Am. Chem. Soc. 105 (1983), pp. 7512–7516.

[21] R.G. Parr and W. Yang, *Density Functional Theory of Atoms and Molecules*, Oxford University Press, New York, 1989.

[22] G.J. Iafrate, K. Hess, J.B. Krieger, and M. Macucci, *Capacitive nature of atomic-sized structures*, Phys. Rev. B 52 (1995), pp. 10737–10739.

[23] J.R. Sabin, S.B. Trickey, S. Peter Apell, and J. Oddershede, *Molecular shape, capacitance, and chemical hardness*, Int. J. Quant. Chem. 77 (2000), pp. 358–366.

[24] M. Macucci, K. Hess, and G.J. Iafrate, *Electronic energy spectrum and the concept of capacitance in quantum dots*, Phys. Rev. B 48 (1993), pp. 17354–17363.

[25] J.C. Ellenbogen, C.A. Picconatto, and J.S. Burnim, *Classical scaling of the quantum capacitances for molecular wire*, Phys. Rev. A 75 (2007), 042102.

[26] G. Polya and G. Szegö, *Annals of Mathematics Studies*, Vol. 27, Princeton University Press, Princeton, NJ, 1951.

[27] J. Gazquez and E. Ortiz, *Electronegativities and hardnesses of open shell atoms*, J. Chem. Phys. 81 (1984), pp. 2741–2748.

[28] J.P. Perdew, *Energetics of charged metallic particles: from atom to bulk solid*, Phys. Rev. B 37 (1988), pp. 6175–6180.

[29] Z.Y. Wang, H.Q. Fan, K.H. Su, and Z.Y. Wen, *Structure and piezoelectric properties of poly(vinylidene fluoride) studied by density functional theory*, Polymer 47 (2006), pp. 7988–7996.